Extreme Water Level Decompositions

Y. L. Firing, J. Aucan, M. A. Merrifield, Department of Oceanography, University of Hawai'i at Mānoa, Honolulu, Hawai'i
and J. M. Becker, Department of Geology and Geophysics, University of Hawai'i at Mānoa, Honolulu, Hawai'i

Abstract

Hourly and daily averaged tide gauge time series are used to determine the primary contributors to high water levels on a station-by-station basis. The water level records are decomposed into tidal, high frequency (e.g. storms, eddies), seasonal, and low frequency (e.g., ENSO) variability and secular trends. The superposition of these components provides visual representations of extreme event climatologies, which in turn help identify the primary causes of extreme water level events at each location. A case study which also examines the role of wave forcing is presented for Midway, Hawaii.

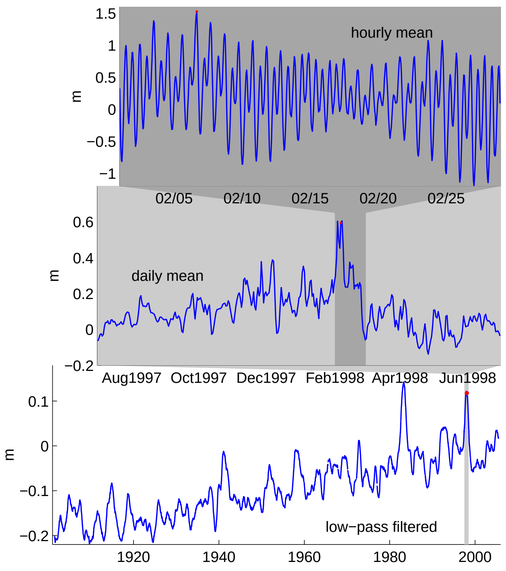

FIGURE 1: Components of an extreme event at San Francisco (February 6, 1998, red dot).

The different components of an extreme event at San Francisco are illustrated in **Figure 1**. The high water level at high tide on February 6, 1998 was caused by a superposition of the 1997-98 El Niño and a storm event.

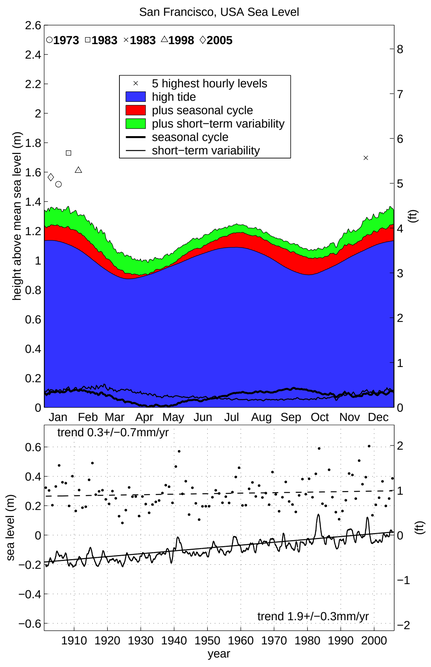

FIGURE 2: Decomposition of San Francisco sea level.

We separate the **San Francisco** timeseries into tidal, short-term, seasonal, and low-frequency components, which are summed to form an extreme event climatology as a function of yearday at this location (**Figure 2**, top panel). The tide component (blue) is defined as the 10% exceedance level for each yearday using the predicted high tide. The seasonal component (red) is the yearday mean sea level. The short-term component (green) is the 10% exceedance level of the high-pass-filtered timeseries (cutoff period $\sim$ 5 months). The five highest recorded hourly values (symbols) occur during winter, as predicted by the climatology, due to storm-induced short-term events combining with the highest tides of the year and a weak seasonal sea level maximum. Higher than average tides in the summer are out of phase with the other components.

The low-pass-filtered timeseries and trend (bottom panel, solid lines) indicate that three of the five highest recorded hourly extremes (top panel) occur during El Niño years (1972-73, 82-83, 97-98). The annual maximum daily mean sea level (dots in time series plot), relative to the long-term mean trend, shows no significant trend in the magnitude of extreme highs at this location. Other stations (**Figures 3 - 7**) have different extreme climatologies.

We attempt to put these and other tide gauge stations into a global context by applying a similar deconstruction (tidal (**Figure 8**), seasonal (**Figure 9**), and short term (**Figure 10**) components) to Topex/Poseidon-Jason sea surface height (SSH) data. Since the 10 day altimeter period undersamples storm-related short-term variability, we have added the same 10% exceedance threshold of daily mean NCEP sea level pressure. The correspondence between the global patterns and tidegauge components is good in most areas.

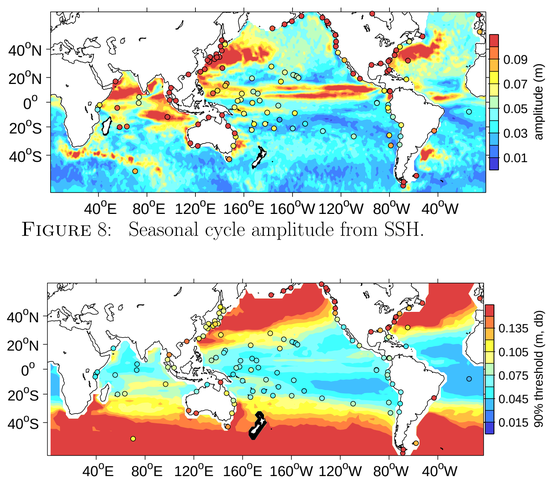

FIGURE 8: Seasonal cycle amplitude from SSH.

FIGURE 9: 90% threshold of high frequency events, from SSH and NCEP sea level pressure.

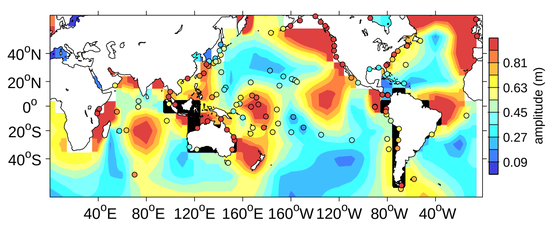

FIGURE 10: 90% threshold of high tide height, from TPXO0.5.

Midway Waves and Water Level

Because tide gauges typically are located in harbors, they do not always capture the wave-driven setup that can dominate coastal water level extremes. As an example of the wave-setup effect, we consider the tide gauge located in the lagoon of Midway atoll (**Figure 11**). Extreme water levels are associated with energetic winter swell events (**Figure 12**). Over a 50 year time span, the predictability of high water level is highest in winter, with wave height the strongest contributor compared to local sea level pressure, wind stress, and mesoscale eddies (**Figure 13**). The number of extreme wave and water level events appears to be correlated with the Southern Oscillation (SOI) and the Pacific Decadal Oscillation (PDO) indices (**Figure 14**). During El Niño (negative SOI) events and positive PDO phases, winter storms are stronger in the North Pacific, resulting in a stronger wave climate at Midway (**Figure 15**). The opposite is true during La Niña and negative PDO phases.

To extend the tide gauge extreme water level climatologies to nearby open coastal regions, future analyses will include the local wave set-up component in more detail.

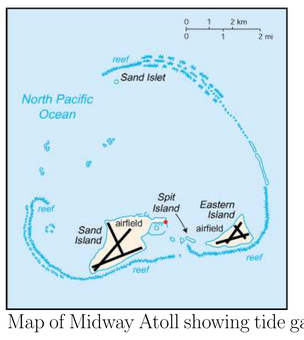

FIGURE 11: Map of Midway Atoll showing tide gauge location (red dot).

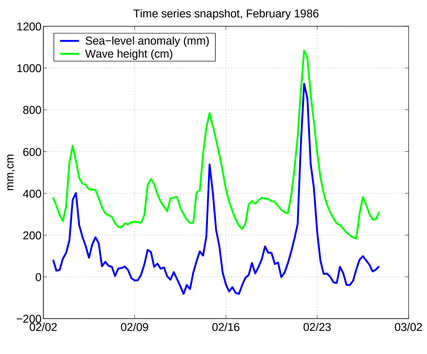

FIGURE 12: Example of wave and water level timeseries showing correspondence.

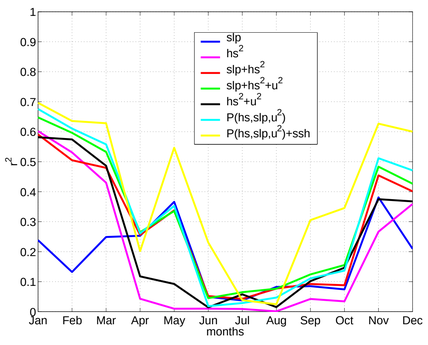

FIGURE 13: Correlation r^2 between Midway sea-level anomaly and various linear regression models for each month. Models use sea level pressure (slp) and significant wave height (hs) from the ERA-40 reanalysis at 28.5°N, 178°W; wind stress (u^2); a polynomial as described in the legend; and T/P sea surface height (ssh).

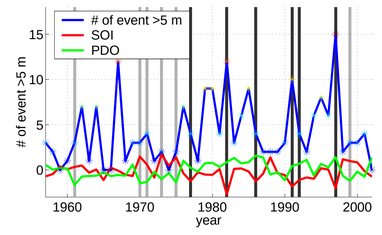

FIGURE 14: Top panel: number of wave events greater than 5 m at Midway between September and April each year, and the Southern Oscillation (SOI) and Pacific Decadal Oscillation (PDO) indices averagedover the same months. Bottom panel: scatter plot of PDO and SOI corresponding to events indicated by colored stars above. Blue lines divide space into four quadrants with an equal number of events in each.

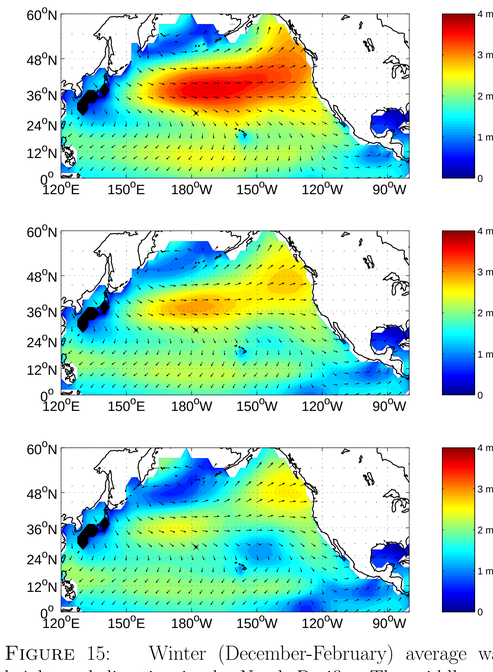

FIGURE 15: Winter (December-February) average wave height and direction in the North Pacific. The middle panel shows the average of all winters 1958-2001; the top panel the average of years when when PDO> 0 and SOI< −1 (corresponding to the lower right quadrant in Figure 15: 1958-59, 1977-78, 1982-83, 1986-87, 1991-92, 1997-98); and the bottom panel the average of years when PDO< −1 and SOI> 0 (corresponding to the upper left quadrant in Figure 15: 1961-62, 1970-71, 1971-72, 1973-74, 1975-76, 1990-91, 1999-2000).

Acknowledgements

Data from the ERA-40 re-analysis was provided by the European Center for Medium-Range Weather Forecasts (ECMWF) data server. Data from the NCEP reanalysis, SOI, and PDO indices were provided by the NOAA-CIRES Climate Diagnostics Center (CDC). Topex/Poseidon data was provided by G. Mitchum, University of Florida. Data from the TPXO0.5 model was provided by G. Egbert and L. Erofeeva, Oregon State University.

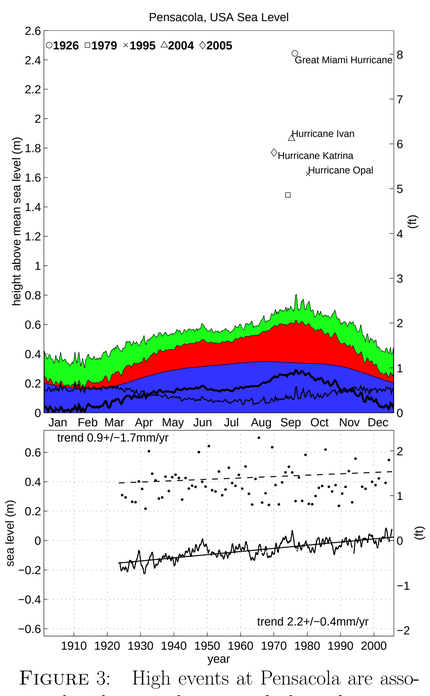

FIGURE 3: High events at Pensacola are associated with tropical storms which tend to occur during the seasonal sea level maximum in August and September.

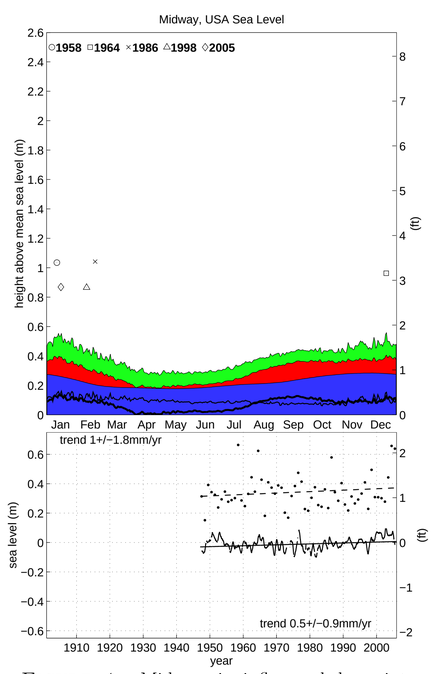

FIGURE 4: Midway is influenced by winter storms and swell events (as discussed in the section on Midway waves and water level).

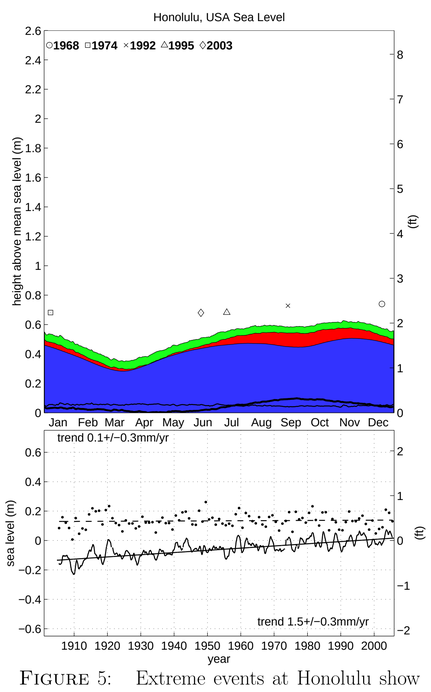

FIGURE 5: Extreme events at Honolulu show a weak seasonal dependence; high water level are often linked with mesoscale eddies that appear at all times of the year.

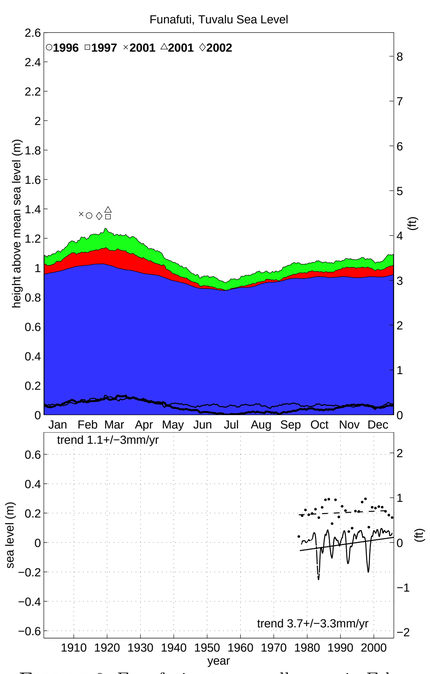

FIGURE 6: Funafuti extremes all occur in February and March, with the combination of a high seasonal cycle and high tide.

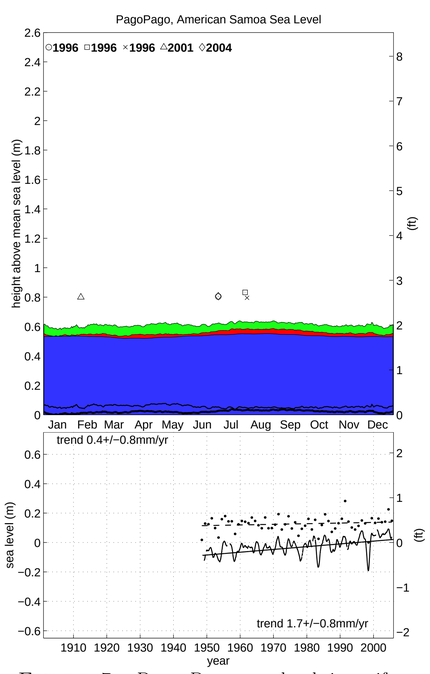

FIGURE 7: Pago Pago sea level is uniform throughout the year in all components.